Temperature dependence of giant magnetoresistance and magnetic properties in electrodeposited Co-Cu/Cu multilayers: The role of superparamagnetic regions

L. Péter,[1,*] Z. Rolik,[1,†] L. F. Kiss,[1] J. Tóth,[1] V. Weihnacht,[1,‡] C. M. Schneider,[2,§] and I. Bakonyi[1]
[1]*Research Institute for Solid State Physics and Optics, Hungarian Academy of Sciences. H-1525 Budapest, P.O.B. 49, Hungary*
[2]*Institute for Solid State Research (IFF-IEE), Research Centre Jülich, D-52425 Jülich, Germany*
(Received 19 October 2005; revised manuscript received 13 March 2006; published 9 May 2006)

We have shown recently that both the magnetization and the magnetoresistance of electrodeposited Co-Cu/Cu multilayers can be decomposed by assuming the presence of both ferromagnetic (FM) and superparamagnetic (SPM) regions in the magnetic layers. In the present work, for two selected samples, one with a large SPM and another one with a large FM contribution to the giant magnetoresistance, low temperature magnetic and magnetoresistance measurements were performed in order to reveal the evolution of the FM and SPM terms with temperature. The average apparent magnetic moment of the SPM regions deduced from the two sets of data showed a good agreement. The role of electrochemical processes in the formation of the SPM regions is discussed. An attempt has also been made to elaborate on some models for the spatial distribution of the constituent elements (Co and Cu) leading to the occurrence of SPM regions. The results are discussed also in the framework of interacting SPM regions.

DOI: 10.1103/PhysRevB.73.174410 PACS number(s): 75.47.De, 75.70.Cn, 75.20.−g, 81.15.Pq

I. INTRODUCTION

It has been reported for several magnetic/nonmagnetic multilayer systems prepared by using a variety of techniques such as sputtering,[1–5] molecular-beam epitaxy (MBE),[6,7] or electrodeposition[8–10] that in samples obtained under certain deposition conditions the magnetization contains, besides a ferromagnetic (FM) magnetization component, a superparamagnetic contribution (SPM) as well. We can visualize the magnetic layers in such multilayers as consisting of both FM and SPM regions whereby the SPM regions are magnetically decoupled from the FM regions of the magnetic layers.

In magnetic/nonmagnetic metallic nanostructures containing both FM and SPM entities, the field and temperature dependence of the giant magnetoresistance (GMR) can be described by the Wiser-Hickey model.[11,12] This model assumes that for a given temperature there is a distribution of magnetic particle sizes with some particles being in the SPM regime and the rest of the particles in the FM regime. With the simultaneous presence of both FM and SPM regions, the GMR may consist of three contributions: (i) $GMR_{SPM\text{-}SPM}$, (ii) $GMR_{FM\text{-}FM}$ and (iii) $GMR_{SPM\text{-}FM}$ $(=GMR_{FM\text{-}SPM})$, whereby a term $GMR_{A\text{-}B}$ refers to magnetoresistance contribution due to a spin-dependent scattering event at the end of an electron path "magnetic region A → nonmagnetic region → magnetic region B."

In recently studied electrodeposited Co-Cu/Cu multilayers,[10] we found that beyond technical saturation of the magnetization at about $H_s = 1.7$ kOe, the field dependence of both the magnetization $M(H)$ and the magnetoresistance $MR(H)$ could be described by the Langevin function $L(x)$ where $x = \mu H/kT$ with μ constituting the average magnetic moment of a SPM region. According to the Wiser-Hickey model,[11,12] the GMR in these Co-Cu/Cu multilayers arises from spin-dependent scattering of electrons which travel through the non-magnetic spacer between two FM regions $(GMR_{FM} = GMR_{FM\text{-}FM})$ or between a FM region and a SPM region $(GMR_{SPM} = GMR_{SPM\text{-}FM} = GMR_{FM\text{-}SPM})$ whichever is the first or second (here, we introduced a simplified notation for those two GMR terms which will be important for our further discussion).

If the FM regions are spatially sufficiently extended (at least in two dimensions such as in multilayers), an electron may undergo two subsequent spin-dependent scattering events in the same FM region. This gives rise to an anisotropic magnetoresistance (AMR) effect[13] well-known for bulk homogeneous ferromagnets. Beyond saturation $(H > H_s)$, the GMR_{FM} and the AMR terms are saturated and, hence, their contributions are constant, apart from a small linear term which is also present in bulk ferromagnets but negligible compared to the other effects in multilayer samples. Therefore, the contribution of the GMR_{FM} and AMR terms cannot be separated from each other at $H > H_s$, and their sum will be denoted as a single MR_{FM} term.

In this manner, one can describe the $MR(H)$ data for magnetic fields $H > H_s = 1.7$ kOe in the form[10]

$$MR(H) = MR_{FM} + GMR_{SPM} \cdot L(x), \tag{1}$$

whereby $MR_{FM} = AMR + GMR_{FM}$ is a constant term. The relative weight of the MR_{FM} and the GMR_{SPM} terms as well as that of the two contributions in MR_{FM} (AMR and GMR_{FM}) do not simply depend on the volume fractions of the two kinds of magnetic region. This is because these weights are also determined by the scattering probabilities in the different regions and by geometric factors, i.e., the shape, relative position, spatial distribution, and the morphology of each region. In Co-Cu/Cu multilayers, the difference between the longitudinal (LMR) and transverse magnetoresistance (TMR) curves is usually not very large (typically 1%); therefore, the observed MR_{FM} term is dominated by the GMR_{FM} contribution.

The above decomposition method can be helpful in analyzing the strongly nonsaturating behavior of GMR curves

observed in many multilayer systems. Recently, we have reported[14] on a room-temperature MR study of electrodeposited Co-Cu/Cu multilayers prepared under a wide variety of deposition conditions. Depending on the specific preparation parameters, large differences were observed in the field dependence of the MR curves, even if the MR(H=8 kOe) values were very similar. In a recent study,[15] the room-temperature magnetoresistance has been decomposed for two selected samples of those series, one with large SPM and another one with large FM contributions to the GMR. In the present work, low temperature (12–300 K) magnetoresistance measurements were performed on the same two samples in order to reveal the evolution of FM and SPM terms with temperature by decomposing the magnetoresistance contributions according to the method described in Ref. 10. In addition, the temperature dependence of the magnetization (M) was also measured.

For both samples, the experimental data revealed the presence of SPM regions in the magnetic layers. The average magnetic moment of these regions decreased nearly linearly for $T \rightarrow 0$ K, both from magnetoresistance and magnetic measurements. The results are discussed also by accounting for an interaction between the SPM entities and by considering the possibility of the occurrence of SPM regions in the form of magnetically separated "islands" in the magnetic layers or interfacial layers with "loose spins."

The paper is organized as follows. In Sec. II, the sample preparation method and the measurement techniques are briefly described. The results of the low-temperature magnetoresistance and magnetic measurements as well as the analysis of these results by taking into account noninteracting SPM clusters are presented in Sec. III. Section IV presents the qualitative elucidation of the sample properties and the influence of the preparation conditions on the properties observed. Then, the model of interacting superparamagnets is applied for the samples presented (Sec. V), while the possible spatial arrangements resulting from this analysis are discussed in Sec. VI. Finally, Sec. VII summarizes the main conclusions of this study.

II. EXPERIMENTAL DETAILS

A. Sample preparation and structural characterization

The sample preparation details have been described previously.[14] An aqueous electrolyte with two solutes ($CoSO_4$ and $CuSO_4$) was used to prepare magnetic/nonmagnetic Co-Cu/Cu multilayers by combining a galvanostatic (G) and a potentiostatic (P) pulse for the deposition of the magnetic and nonmagnetic layer, respectively (this pulse combination was denoted earlier as the G/P mode[14]). The composition of the magnetic layer (often referred to later as a Co layer) was $Co_{95}Cu_5$.[16] The electrodeposition was performed in a tubular cell ensuring a lateral homogeneity of the deposition current density over the cathode area. The layer thicknesses were controlled via the pulse lengths and, from the charge deposited during the pulse, the nominal layer thicknesses were determined. After deposition, the multilayers with a bilayer number of 300 were peeled off mechanically from the Ti sheet substrate.

For the present low-temperature study, two samples prepared during the course of the work described in Ref. 14 were selected. The nominal thicknesses of multilayer V4 were Co(3.4 nm)/Cu(0.2 nm) and those of multilayer V6 were Co(3.4 nm)/Cu(2.5 nm). Under the applied deposition conditions,[14] a strong dissolution of the Co layer occurs during the Cu deposition pulse.[17] As a consequence, the actual Co-layer thickness becomes smaller and the actual Cu layer becomes larger than the nominal thicknesses. From a chemical analysis of the overall composition of Co-Cu/Cu multilayer deposits,[10,14,18] the actual layer thicknesses can be reliably estimated. For the currently investigated two multilayers, the composition analysis yielded the actual layer thicknesses Co(2.0 nm)/Cu(1.6 nm) for sample V4 (Ref. 14) and Co(2.1 nm)/Cu(3.8 nm) for sample V6.[18]

According to a separate study[18] by x-ray diffraction (XRD) and transmission electron microscopy (TEM), the electrodeposited Co-Cu/Cu multilayers V4 and V6 exhibited a face-centered cubic (fcc) structure. The XRD patterns revealed a strong (111) texture along the growth direction. Cross-sectional TEM imaging[18] clearly showed a well-defined multilayer structure for sample V4 and also for another multilayer with very similar nominal thicknesses as sample V6.

B. Mesasurement of magnetoresistance and magnetic properties

The MR data were measured on 1 to 2 mm wide strips with the four-point-in-line method in magnetic fields between −8 and +8 kOe in the field-in-plane/current-in-plane geometry. The longitudinal magnetoresistance (LMR; field parallel to current) component was recorded for both samples from 12 to 300 K in a closed-cycle He cryostat. The following formula was used for calculating the magnetoresistance ratio: $\Delta R/R_0=[R(H)-R(0)]/R(0)$ where $R(H)$ is the resistance in the magnetic field H and $R(0)$ is the resistance when $H=0$.

A superconducting quantum interference device (SQUID) magnetometer was used to measure the variation of the in-plane magnetization with temperatures from 12 to 300 K up to H=50 kOe on the same strips of samples V4 and V6 which were used for the MR measurements.

III. EXPERIMENTAL RESULTS AND DATA ANALYSIS WITH THE MODEL OF INDEPENDENT SPM REGIONS

A. Magnetoresistance

Samples V4 and V6 were selected for the low-temperature study on the basis of their strongly different MR behavior at room temperature as reported previously.[15] The longitudinal MR curves were measured at several temperatures down to 12 K for both samples and they are displayed in Fig. 1. For sample V4, the MR curves do not show saturation up to

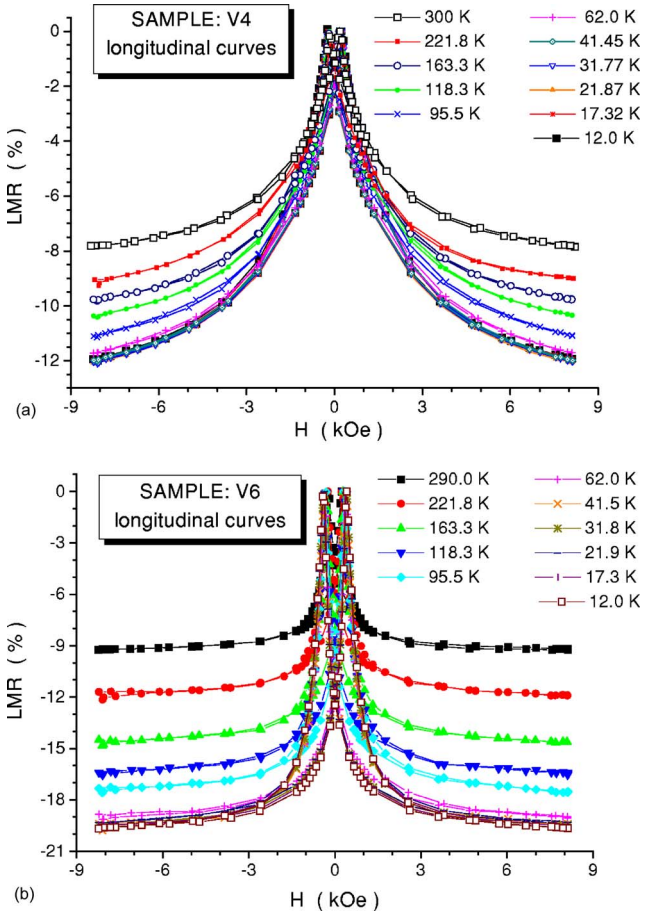

FIG. 1. (Color online) Temperature dependence of the longitudinal magnetoresistance for sample V4 (a) and sample V6 (b).

8 kOe [Fig. 1(a)], whereas for sample V6 the MR change becomes very small beyond about 2 kOe [Fig. 1(b)]. This indicates a predominant SPM and FM behavior, respectively.[10,15]

A decomposition analysis of the MR data was performed at each temperature in the way described in Ref. 10. Briefly, for $H > H_S = 1.7$ kOe the magnetoresistance as a function of the external magnetic field was fitted with Eq. (1) where $x = \mu H/kT$. The saturation values of the total LMR (MR_s) and its SPM and FM components are shown in Fig. 2(a) as a function of temperature. These data reveal a strong difference in the temperature evolution of the GMR for the two selected multilayers. Whereas at room temperature the total magnetoresistance values are nearly the same for both samples, the increase of the magnetoresistance toward low temperatures is much larger for sample V6. The decomposition analysis furthermore reveals that in both samples the FM and SPM components of the GMR increase in line with each other. As a consequence of this behavior, the relative weight of the SPM contribution to MR hardly changes with temperature as shown in Fig. 2(b). This trend leads one to the conclusion that the relative importance of the various spin-dependent scattering events is independent of temperature.

Figure 2(c) shows the temperature dependence of the average moment μ of a SPM region. For a given temperature, the average SPM moment as obtained from the MR measurements by assuming noninteracting SPM regions is larger for sample V6 than for sample V4. The ratio of the moments established for samples V4 and V6 is fairly independent of temperature, as seen from the data in the inset of Fig. 2(c). The two samples exhibit a similar behavior in that μ decreases strongly with decreasing temperatue as is observed also in MBE-grown Co/Cu multilayers.[19,20]

The temperature evolution of the MR peak position (H_p) is shown for both samples in Fig. 2(d). An approximately linear increase of the peak position with decreasing temperature can be noticed.

B. Magnetic properties

The results of magnetic measurements performed at three temperatures are shown for sample V4 in Fig. 3. The results of the magnetic measurements for sample V6 were qualitatively similar to those of sample V4. The magnetization values were referred to the magnetic layer only, by using the actual layer thicknesses as specified in Sec. II A. Data in the low-field range [Fig. 3(a)] indicate magnetic hysteresis with coercive field (H_c) values increasing with decreasing temperature [see Fig. 2(d)]. An overview of the magnetization data for both samples in the entire temperature and magnetic field range studied can be seen in a reduced magnetization diagram in Fig. 4.

It can be seen from Fig. 2(d) that for sample V4 the field values at the resistance maximum (H_p) and the coercivity (H_c) values obtained from magnetization curves coincide over the whole temperature range investigated. However, the coercive field for sample V6 is by about 60 Oe smaller throughout the whole temperature range than the magnetic field at which the MR peak exhibits the maximum. This difference indicates that the magnetically most disordered state for sample V4 is achieved when the sample is in a state of zero magetization. This feature of sample V4 is in agreement with the SPM behavior. In contrast to sample V4, sample V6 needs a significantly larger opposite field to achieve the maximum of the magnetic disorder than the coercive field. This feature of sample V6 can be related to the dominance of the FM contribution in the magnetoresistance. It also needs to be emphasized that while the coercive field characterizes the random magnetization direction in the entire sample, the maximum position of the magnetoresistance curves is an indication of the most disordered magnetization configuration within the spin diffusion length of the electrons. Obviously, these terms can be either very close to each other or very different, depending on the spatial arrangement of each magnetic region.

The magnetization curves for intermediate magnetic fields are shown in Fig. 3(b). Along the line of the former discussion about the decomposition of the magnetoresistance, we assume also for the analysis of the magnetization that it consists of a FM and a SPM contribution. Specifically, for magnetic fields $H > H_s \approx 1.7$ kOe, i.e., where the hysteresis loops approximately closed, the magnetization is fitted by using the following formula:

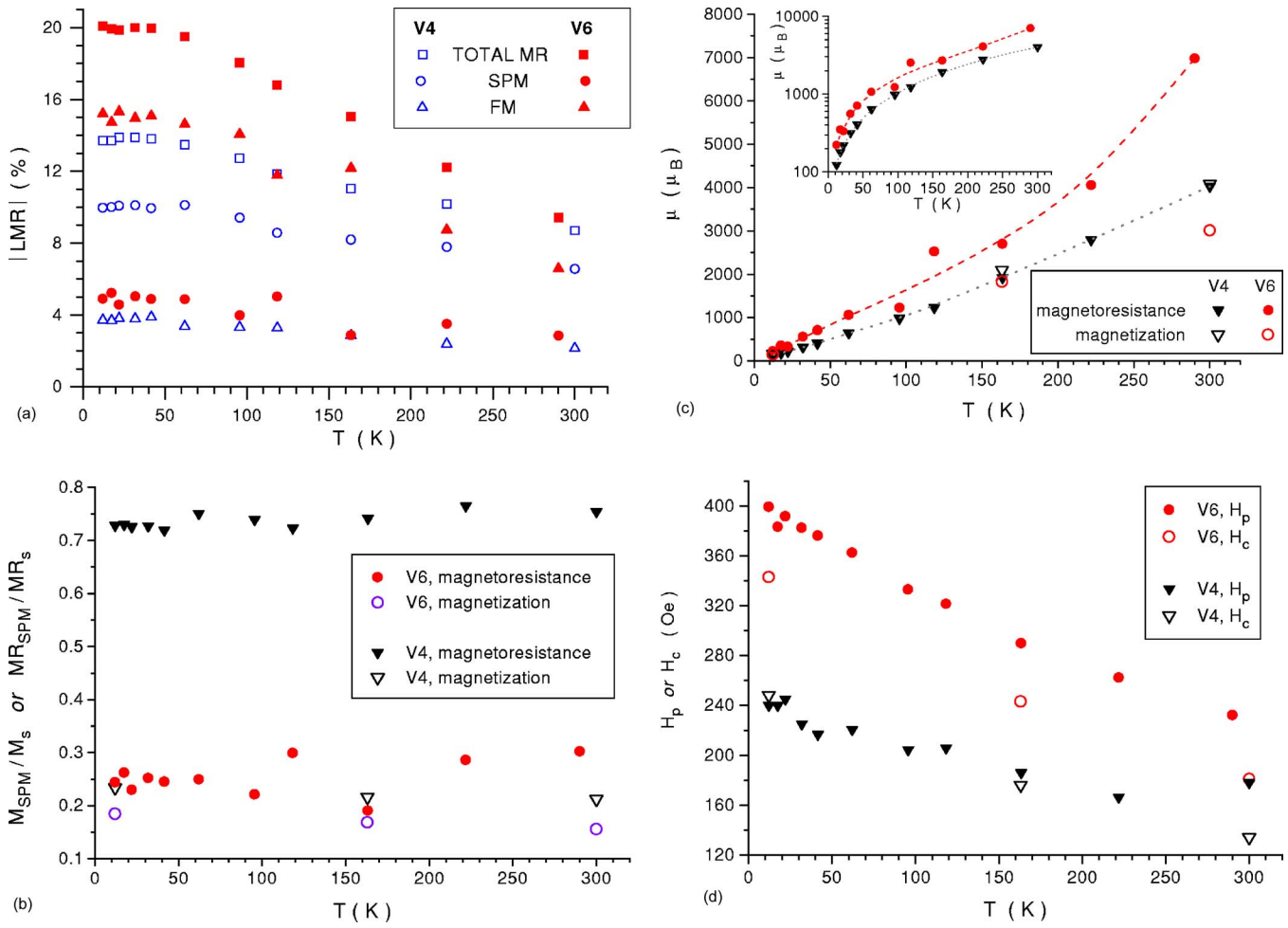

FIG. 2. (Color online) Temperature dependence of various magnetoresistance and magnetic parameters determined for both samples V4 and V6: (a) total (saturated) longitudinal magnetoresistance MR_s and its FM and SPM contributions; (b) fractional SPM contribution to the saturation magnetoresistance MR_s and saturation magnetization M_s; (c) average magnetic moment μ of SPM regions (the inset shows the same data as the main frame except that they are plotted on a logarithmic vertical scale in order to better demonstrate that the ratio of the average SPM moments for the two samples V4 and V6 is fairly independent of temperature); (d) magnetoresistance peak position H_p and coercive field H_c. Lines in (c) are only a guide for the eye to follow the trend of the SPM moment as derived from magnetoresistance data.

$$M(H) = M_{\mathrm{FM}} + n\mu L\left(\frac{\mu H}{kT}\right), \tag{2}$$

where M_{FM} is the saturation magnetization of the FM component and n is the SPM cluster density. The values of the cluster moment μ and the saturation value of the total magnetization (M_s) are specified in Fig. 3(b). The shape of the magnetization loop indicates that the major magnetization process is related to the FM part. This is in contrast to the magnetoresistance [see Fig. 2(b)] for which the SPM contribution amounted to some 75% of the total GMR. This very large difference is mainly due to the fact that the magnetization ratio is determined by the volume fractions of the two components only whereas for the GMR the magnitude of the FM and SPM contributions strongly depends also on the mutual spatial arrangement of the two kinds of regions. It is also important to note that the GMR is mainly governed by electron transitions across magnetic/non-magnetic interfaces.

Since $M_s(0\ \mathrm{K}) = 166$ emu/g for face-centered cubic Co,[21] from the Slater-Pauling curves we can estimate $M_s(0\ \mathrm{K}) = 161$ emu/g for the magnetization of the $Co_{95}Cu_5$ alloy which is the actual composition of our magnetic layer. This is somewhat smaller than the saturation magnetization $M_s(12\ \mathrm{K}) = 165$ emu/g of the magnetic layer of sample V4 (Fig. 3), the latter value being obtained by assuming the actual layer thicknesses $Co_{95}Cu_5$(2.0 nm)/Cu(1.6 nm). The slight difference can be explained if we assume that the actual magnetic layer thickness is by 3% higher than the value specified above. This means, on the other hand, that the sublayer thicknesses deduced from the chemical analysis data for sample V4 (Ref. 14) are, indeed, fairly close to the true thickness values.

A fitting of the magnetization data with Eq. (2) was performed also for sample V6 and the derived average SPM magnetic moment data are included in Fig. 2(c). As to the saturation magnetization of the magnetic layer for sample V6, we obtained $M_s(12\ \mathrm{K}) = 182$ emu/g by using the actual thickness values $Co_{95}Cu_5$(2.1 nm)/Cu(3.8 nm). Here the de-

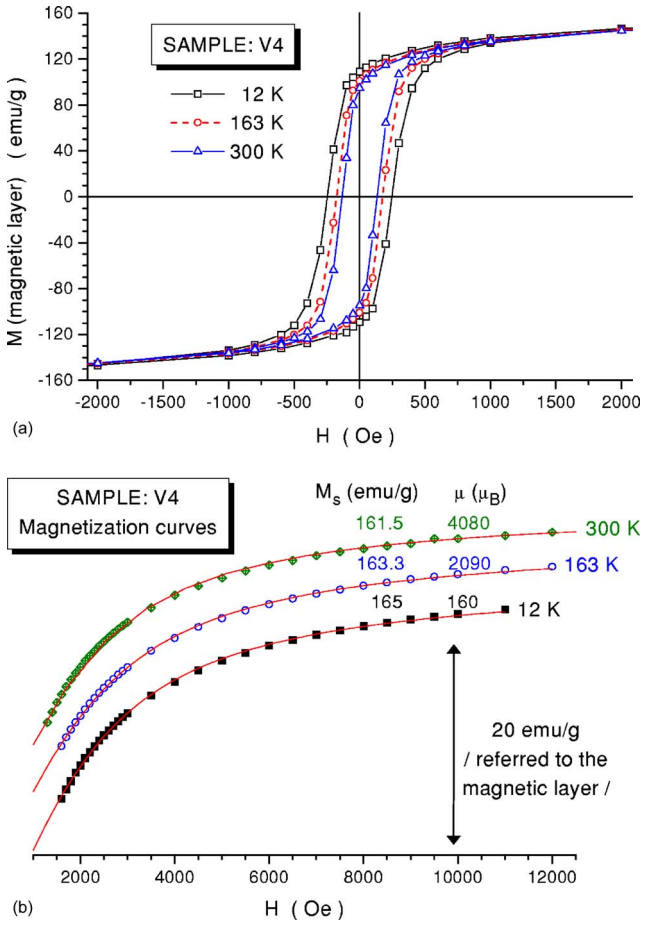

FIG. 3. (Color online) (a) Magnetic hysteresis loops at three temperatures for multilayer sample V4 with the magnetization referred to the unit mass of the magnetic layer by using the actual layer thicknesses; (b) magnetization curves for sample V4 at three temperatures for intermediate magnetic fields where the evolution of the SPM magnetization contribution can be observed. The solid lines represent Langevin fits to the data. The values of the saturation magnetization referred to the magnetic layer and the average SPM magnetic moment are attached to the data curves for each temperature.

viation from the expected $M_s(0\ \mathrm{K})=161$ emu/g value of $Co_{95}Cu_5$ is relatively high; however, even in this case the deviation can be explained if we assume that the actual magnetic layer thickness is by 13% higher than the value specified above which is still reasonable. This slight difference will not affect our further discussion.

IV. DISCUSSION OF THE PROPERTIES OF THE MULTILAYER SAMPLES

A. Comparison of the samples subject to this study

According to the results described above, multilayers V4 and V6 exhibit very different GMR behavior in spite of the fact that their room-temperature GMR values as measured in a magnetic field of 8 kOe are very similar. The magnetoresistance data indicate a dominance of the SPM contribution to the GMR for sample V4 in contrast to sample V6 in which

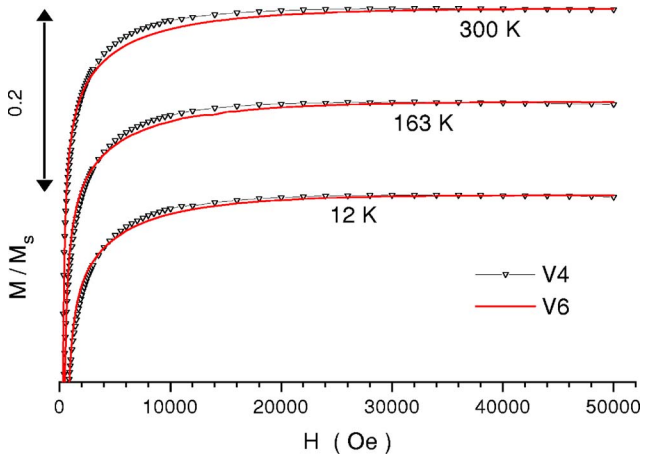

FIG. 4. (Color online) High-field section of the reduced magnetization curves for samples V4 and V6 at three temperatures. Note that the magnetization curves taken at different temperatures have been shifted vertically with respect to each other in order to better display them for both samples.

the FM contribution dominates. On the other hand, Fig. 2(b) reveals that in the total magnetization the SPM contribution differs only slightly for the two samples, amounting to about 20% for both multilayers. This is further exemplified in Fig. 4 where their magnetization curves at high field are compared for the three temperatures investigated.

The size of the average magnetic moment μ of SPM regions agrees well for sample V4 when the values derived from magnetic and magetoresistance data are compared. On the other hand, for sample V6 the μ values from MR data are higher and those from the magnetic data are smaller than the corresponding values of sample V4 [Fig. 2(c)].

The explanation of the observed differences should be sought in the details of the underlying electrochemical processes governing the morphology of the multilayer growth. All the preparation parameters were identical except for the nominal Cu layer thickness.

For multilayer V4 (nominal magnetic/nonmagnetic layer thickness: 3.4 nm/0.2 nm), the Cu layer with a final thickness of 1.6 nm is built up almost exclusively at the expense of the dissolution[17] of the originally deposited magnetic Co-Cu layer (the latter being reduced to an average thickness of about 2 nm). Such a consumption of the magnetic layer occurs randomly over the cathode area and this leads to a strong fluctuation of the magnetic layer thickness. At the extreme, such fluctuations may lead to a discontinuity of the magnetic layer at some places and, thus, SPM regions can form which are magnetically decoupled from the FM part of the magnetic layers. This tendency may be further enhanced as a result of some unavoidable degree of intermixing due to the random Co-dissolution and Cu-deposition processes which may take place during almost the total duration of the Cu deposition pulse. These features may well explain the dominance of the GMR_{SPM} term in the magnetoresistance of multilayer V4.

This picture is in accordance with our recent work on electrodeposited Co-Cu/Cu multilayers[22] where we have concluded that below about 2.5 nm effective thickness the

Cu layers are not yet continuous and this also strongly contributes to a fragmentation of the magnetic layers into SPM type regions. Thus, the preparation conditions of sample V4 having an average Cu layer thickness of 1.6 nm promote the formation of a granular type quasi-multilayer structure in which both FM and SPM regions can occur in the magnetic layer.

The situation is quite different for multilayer V6 for which the nominal magnetic/nonmagnetic layer thicknesses are 3.4 nm/2.5 nm and the actual layer thicknesses are 2.1 nm/3.8 nm. Again with reference to our recent work,[22] for Cu layer thicknesses above about 2.5 nm as is the case here the Cu layer is definitely continuous and this favors the formation of continuous magnetic layers even at thicknesses where their fragmentation occurs at thinner Cu layers. Therefore, the occurrence of dispersed SPM regions in the magnetic layers is less favored what is reflected in the fact that the GMR_{SPM} contribution is much smaller than for multilayer V4. Also, the Cu layer thickness is much larger for sample V6 which may well lead to a "leveling" effect and, thus, each subsequent Co layer may start to grow on a much smoother surface and may become more uniform. It will, thus, be less inhomogeneously consumed during the Cu deposition pulse than for multilayer V4.

These considerations are further supported by the coercive field data. We have measured the room temperature low-field hysteresis loop for a bulk $Co_{95}Cu_5$ alloy obtained by direct-current electrodeposition at the same current density as used for the magnetic layer in the multilayer structure and the room-temperature coercive field was about 30 Oe. In view of this result, the high coercive field values for sample V6 indicate the presence of continuous and well-separated thin magnetic layers in the multilayer structure as found previously[22] and is well-known for thin ferromagnetic films.[23] On the other hand, the typically 50% lower coercive field values for sample V4 with an effective (average) magnetic layer thickness identical to that of sample V6 hint toward larger effective magnetic layer thicknesses at least in some areas. This suggests the presence of larger magnetic regions percolated over several layers through the pinholes in the discontinuous Cu layers.

B. Comparison of the temperature dependence of the magnetoresistance of electrodeposited Co-Cu/Cu and Ni-Cu/Cu multilayers

For both Co-Cu/Cu multilayers described in this study, a significant increase of the MR values with decreasing temperature can be observed whereas the overall shape of the room-temperature MR curves is retained. This is in contrast to the case of electrodeposited Ni-Cu/Cu multilayers for which even the shape of the MR curves changed significantly with temperature.[9] The most probable reason for this difference is that for the Ni-Cu/Cu system all the SPM regions become FM regions at the lowest measuring temperature whereas for the Co-Cu/Cu system some regions always remain in the SPM state.

In the case of the Ni-Cu/Cu multilayers, the occurrence of a SPM-FM transition (blocking) at low temperature has at least two reasons. On the one hand, by cooling the sample, the measuring temperature becomes lower than the blocking temperature of some SPM regions (this effect can equally work for both Ni-Cu/Cu and Co-Cu/Cu multilayers). On the other hand, however, one has to take into account also a possible paramagnetic-ferromagnetic transition of the boundary separating the SPM and FM regions. By comparing the composition dependence of the Curie temperature of the Ni-Cu and Co-Cu alloys, one obtains that $dT_C/dc = 11.8$ K/at. % for the Ni-Cu system,[24] while for metastable Co-Cu alloys the same data is 30.8 K/at. %.[25] This means that the composition interval that can undergo a paramagnetic-ferromagnetic transition during the same temperature change is 2.6 times higher for the Ni-Cu system than for the Co-Cu system. It can also be assumed that for Ni-Cu samples the local composition may vary continuously because of the miscibility of the components. In contrast, the very limited miscibility in the case of the Co-Cu system may result in precipitates, and the boundary regions are probably so Cu rich that they cannot undergo a PM-FM transition at any temperature. Hence, a PM-FM transition of the boundary regions occuring with temperature in the Co-Cu system is much less likely than for the Ni-Cu system.

V. DATA ANALYSIS: THE MODEL OF INTERACTING SPM REGIONS

The decomposition of both magnetic and magnetoresistance data shows that the SPM-like behavior of the samples is retained at low temperature as if the magnetic moment of the SPM regions could not be blocked even at the lowest temperature applied. At the same time, the apparent average moment of the SPM regions decreases, implicitly implying the gradual blocking of smaller and smaller clusters with decreasing temperature. Since the redistribution of the atoms at low temperature leading to a fragmentation of SPM regions can be completely excluded, resolving this discrepancy requires the simple picture of independent FM and SPM regions to be modified.

Magnetic dipolar interactions between the SPM regions themselves and eventually between the SPM and the FM regions can be effective if these regions are sufficiently close to each other. Kechrakos and Trohidou have shown by theoretical modeling[26] that dipolar interactions between Co particles with SPM behavior in a granular Co(Cu) system give rise to a much lower rate of approach to saturation of both magnetization and magnetoresistance than in the absence of the interaction. Furthermore, Allia *et al.* have demonstrated[27] that the magnetization curves of an assembly of interacting SPM particles retain the Langevin-like character but meanwhile the apparent size of the SPM regions becomes much smaller than the real one.

The analysis of the result of the Langevin function fitting procedure shows that measurements at a single temperature cannot reveal whether the Langevin-like behavior is caused by interacting or noninteracting regions. The investigation of the temperature dependence of magnetization and magnetoresistance is a unique tool to discriminate between the two cases.

It was demonstrated[27] that the interaction between SPM regions can give rise to magnetic hysteresis as well. Hence, the decomposition of the FM and SPM contributions certainly results in a distorted field dependence of the FM component because in this way the hysteresis is entirely ascribed to the FM component. Nevertheless, in the authors' view this deficiency does not impact the importance and validity of the decomposition method.

Allia *et al.*[27] have dealt with the quantitative description of the magnetization behavior of the assembly of SPM particles. The deviation from the noninteracting behavior was taken into account by the modification of the argument of the Langevin function. Using the notations in the present work, the magnetization is described in this model in the following way:

$$M(H) = M_{\mathrm{FM}} + n'\mu' L\left(\frac{\mu' H}{k(T+T^*)}\right), \tag{3}$$

where n' and μ' are the actual SPM particle density and magnetic moment. These quantities obviously have different values than the apparent n and μ which latter values were derived by using $T^*=0$ while the $\mathrm{M_{SPM}}=n'\mu'$ product remained unchanged. The introduction of the T^* term was justified[27] with the argument that the dipolar interaction exerts disorder, as opposed to the ordering effect of the external field, and hence it plays a similar role as the increase in temperature. However, we should keep in mind that although T^* is formally like a temperature parameter, it is better to adopt the view of kT^* corresponding to a disordering energy due to SPM dipolar interaction.

The magnetoresistance fitting function also needs to be modified accordingly

$$\mathrm{MR}(H) = \mathrm{MR_{FM}} + \mathrm{GMR_{SPM}} L\left(\frac{\mu' H}{k(T+T^*)}\right)$$

$$= \mathrm{MR_{FM}} + \mathrm{GMR_{SPM}} L\left(\frac{H}{k\lambda}\right), \tag{4}$$

where both the meaning and the value of $\mathrm{MR_{FM}}$ and $\mathrm{GMR_{SPM}}$ are identical to those used in Eq. (1), but μ' had to be adjusted to T^* and we introduced the notation $\lambda = T^*/\mu' + T/\mu'$. The simplicity of this method allows one to calculate T^* and μ' from both magnetization and magnetoresistance data, without exactly specifying the magnetization ratio of the FM and SPM fractions.

In principle, the temperature dependence of λ could help to identify μ' and T^*. By assuming that $\mu' \neq f(T)$, $T^* \neq f(T)$ and extrapolating λ to $T=0$ K, one may get T^*/μ' while the slope of the $\lambda(T)$ function yields $1/\mu'$. The $\lambda(T)$ function for the samples V4 and V6 is displayed in Fig. 5. It can be seen that the data points are very scattered. Besides the possible size distribution of the SPM regions (which is neglected in the analysis), one can attribute the errors to the fact that in the case of multilayers, the SPM component has to be separated from a FM contribution. The presence of two types of magnetic regions surely increases the uncertainty of all parameters, especially as compared to a similar analysis of granular materials where all the magnetization can originate from SPM regions only. The uncertainty is so high in this case that even the overall trend is just opposite to what was expected: The λ values are smaller at room temperature than below 50 K. Only the low-temperature region exhibits a linear temperature dependence with a positive slope. The μ' and T^* parameters estimated from the linear sections for both samples V4 and V6 are also indicated in Fig. 5. It can be seen that μ' values are just slightly higher than the values obtained from the conventional Langevin fit to the room temperature data. At low temperatures ($T<50$ K), however, the μ' values indicate by about an order of magnitude larger magnetic moments than the values obtained with the model of noninteracting SPM regions in the same temperature range. At the same time, the parameter T^* is well above the temperature range investigated, especially for sample V4 in which the SPM behavior is dominant.

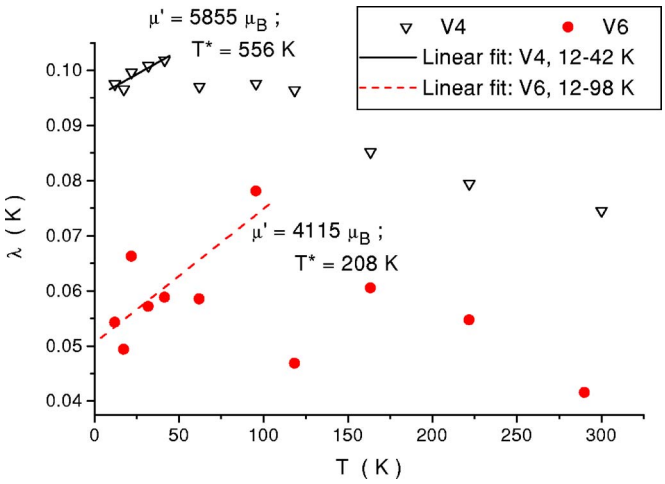

FIG. 5. (Color online) Parameter λ as a function of temperature as obtained from magnetoresistance data. For the definition of λ, see Eq. (4). The values of μ' and T^* for each sample as determined from the low-temperature linear sections (dashed lines) are also indicated.

If T^* is high enough as compared to the measuring temperature, the shape of the $M(H)$ curves becomes independent of the temperature [see Eq. (3)]. It is remarkable that the temperature intervals in which the data can be fitted to a straight line in Fig. 5 coincides with the interval in which the magnetoresistance curves exhibit the same shape (Fig. 1). This supports that the model used can be applied in a limited temperature interval only, and the temperature dependence of μ' and/or T^* becomes significant above a particular temperature.

VI. CONSIDERATIONS ON THE POSSIBLE SPATIAL ARRANGEMENT OF SPM REGIONS

A. Island model of the SPM regions

It has remained an open question as to where the SPM regions are located with respect to the FM parts of the magnetic layers. In Fig. 7 of Ref. 9, we have visualized the SPM regions as being isolated islands within the magnetic layer plane separated from the FM regions by nonmagnetic re-

gions which prevent a coupling of the two kinds of magnetic entities via direct exchange interaction. In this model, we considered the SPM regions as extending from one nonmagnetic layer to the next one, through the entire thickness of the magnetic layer. This view is supported by our experience that the SPM magnetic moment size was usually found to be proportional to the magnetic layer thickness in our electrodeposited Co-Cu/Cu multilayers.[28]

A knowledge of the saturation magnetization data (Fig. 4) and the composition dependence[25] of the saturation magnetization of homogeneous Co-Cu alloys yields an opportunity to estimate the thickness of the nonmagnetic border between the FM parts of the magnetic layers and the SPM islands. By using the average SPM moment size obtained from the Langevin fit [Fig. 2(c)], we arrived at such small border thicknesses that cannot act as preventing a direct coupling between the SPM regions. On the other hand, if the average SPM moment size is assumed to be sufficiently large (typically in excess of 10^4 μ_B) then the resulting nonmagnetic border thickness is already in a range that can effectively prevent a direct coupling between the neighboring SPM moments. These moment values are about one order of magnitude higher than the apparent SPM moment sizes obtained with the simple Langevin fit. This ratio of the actual and apparent SPM moments is in agreement with the analysis carried out in Sec. V on the basis of the model of Allia *et al.*[27] for interacting SPM clusters.

The interaction of the SPM regions, especially when it is extended over several magnetic layers, may lead to the situation that the network of interacting SPM clusters becomes spatially more extended than the continuous FM regions. Hence, consecutive electron scattering events within the same "interaction region" (though not in the same SPM cluster) are possible. This assumption may explain the strange experience that the decomposition of the LMR and TMR curves usually leads to an identical FM component while the SPM contribution of the TMR curve is higher than that of the LMR curve. Apparently, they appear as if the AMR effect were efficient for SPM components only.

B. Interfacial layer model of the SPM regions

Another possibility in accounting for a SPM contribution is to assume that such regions with loose magnetic moments resulting in strongly nonsaturating magnetoresistance curves are situated between the FM "core" of the magnetic layers and the nonmagnetic layers. A sketch of such a situation was shown in Ref. 15. The strong mixing effect of the simultaneous Co dissolution and Cu deposition processes could contribute to the formation of such interfacial "loose-spin" regions but the problem remains how to decouple them magnetically from the FM core of the magnetic layers. A decoupling can occur via a nonmagnetic (Cu-enriched) region or due to the reduced exchange coupling between interfacial magnetic spins with respect to the interaction between atoms in the FM core. As to the latter possibility, it was seriously considered theoretically,[29] and experimental evidence for surface loose spins also seems to exist.[30] The possibility of a different magnetic behavior of surface spins due to the lower coordination has been considered in attempts to explain the anomalous magnetization characteristics of oxide nanoparticles.[31] Along these lines, we might imagine a reduced exchange interaction at the surfaces of the magnetic layer in our multilayers as well, which could then result in a partial decoupling of these surface loose spins from the FM core of the magnetic layers.

It is very difficult to construct a viable model for the component distribution if the SPM behavior is attributed to loose spins. If the thickness of the interfacial region involving loose spins is taken as 0.4 nm (about two atomic layers), one can calculate that one of the two interfaces of a particular magnetic layer has to be entirely occupied by this interfacial layer. However, if this interfacial layer is continuous, it is difficult to understand how the surface spins can be decoupled from the rest of the magnetic layer. The presence of Cu atoms in the magnetic layer is also insufficient to form a monatomic separator layer between the FM core and the surface SPM regions.

VII. SUMMARY

In this paper, extending our previous work,[10] we discussed the GMR behavior of electrodeposited Co-Cu/Cu multilayers by taking into account that the magnetic layers are not fully ferromagnetic but also contain regions exhibiting SPM character. According to the Wiser-Hickey model,[11,12] in such cases the GMR may contain, besides the usual GMR_{FM} term, a contribution GMR_{SPM} with a strong field dependence described by the Langevin function $L(x)$ which arises from spin-dependent scattering events involving a FM region and a SPM region.

The temperature dependence of the magnetoresistance and magnetic properties was studied and analyzed here for two electrodeposited Co-Cu/Cu multilayers with either large or small SPM contribution to the GMR. The observed magnetoresistance could be decomposed into a FM and a SPM term by the method described in Ref. 10 along the lines of the Wiser-Hickey model.[11,12] The average apparent size of the SPM regions from the GMR and the magnetization data was found to be in good agreement, including even their temperature dependence when the dominant contribution to the electron scattering was of the SPM origin. It should be noted that such a decomposition analysis can, of course, be well applied to multilayers prepared by other techniques.

The experimental data on the multilayers investigated here unambiguously revealed the presence of SPM regions which are magnetically decoupled from the FM parts of the magnetic layers. The analysis of our results was extended to the case when the SPM regions exhibit a dipolar coupling with each other as suggested previously for granular alloys.[26,27] However, it is not at all easy to establish the location of the magnetically decoupled SPM regions. We have discussed the possibility of magnetically isolated SPM islands within the magnetic layer plane on the one hand and of "loose-spin" interfaces with SPM behavior between the magnetic and nonmagnetic layers on the other hand. In the present samples, the Co dissolution process can lead to layer thickness fluctuations which, at the extreme, can result in a

complete dissolution of the magnetic layer at some places. Since solute Cu atoms strongly reduce the magnetization of Co metal, a strong Cu enrichment at some places of the magnetic layer can also result in the formation of nonmagnetic regions. By assuming a spontaneous segregation of Co and Cu atoms in the magnetic layer, one can imagine some processes leading to the appearance of SPM islands.

Results on electrodeposited Co-Cu/Cu multilayers prepared under conditions completely excluding the Co dissolution process[28] indicate the presence of a SPM contribution to GMR even in such cases. This hints toward an explanation that some surface loose spins may also be responsible for the occurrence of a nonsaturating GMR in these multilayers. A further support in this respect is that a Langevin type GMR behavior was reported on an MBE-grown Co/Cu multilayer[19,20] on which the atomic resolution TEM study revealed a fairly perfect multilayer structure. High MR saturation fields of about 40 kOe were observed also in other MBE-grown Co/Cu multilayers under certain conditions.[32]

Further sophisticated local structure and chemical analysis techniques, such as three-dimensional (3D) atom probe topography methods,[33,34] should be used to decide between the possible spatial arrangements for the SPM regions (separated islands or interfacial loose-spin layers). We have elaborated on some models for the spatial distribution of Co and Cu in an attempt to give an account of the observed magnetic and MR behavior in terms of separated SPM islands. However, there have still remained serious controversies concerning the interpretation of various datasets in this picture. Since there are indications also for an interfacial location of the SPM regions, further studies are evidently required to clarify which of these two models applies.

ACKNOWLEDGMENTS

This work was supported by the Hungarian Scientific Research Fund (OTKA) through Grant No. T037 673 and No. T047 094 and by the Sonderforschungsbereich, Germany through Grant No. SFB 422. The closed-cycle He cryostat was kindly donated by the Humboldt Foundation, Germany.

*Corresponding author. Email address: lpeter@szfki.hu
†Undergraduate student at Eötvös University, Budapest during the course of this work. Present address: Eötvös University, Department of Theoretical Chemistry, Budapest, Hungary.
‡On leave from the Leibniz Institute for Solid State and Materials Research (IFW), Dresden, Germany. Present address: Fraunhofer Institute for Material and Beam Technology, Dresden, Germany.
§Formerly at: Leibniz Institute for Solid State and Materials Research (IFW), Dresden, Germany.

[1] M. Wu and W. Abdul-Razzaq, Phys. Rev. B **42**, 4590 (1990).
[2] T. Lucinski, F. Stobiecki, D. Elefant, D. Eckert, G. Reiss, B. Szymanski, J. Dubowik, M. Schmidt, H. Rohrmann, and K. Roell, J. Magn. Magn. Mater. **174**, 192 (1997).
[3] F. Spizzo, E. Angeli, D. Bisero, P. Vavassori, and F. Ronconi, Appl. Phys. Lett. **79**, 3293 (2001).
[4] F. Spizzo, E. Angeli, D. Bisero, P. Vavassori, and F. Ronconi, J. Magn. Magn. Mater. **242–245**, 473 (2002).
[5] P. Vavassori, F. Spizzo, E. Angeli, D. Bisero, and F. Ronconi, J. Magn. Magn. Mater. **262**, 120 (2003).
[6] J. Xu, M. A. Howson, B. J. Hickey, D. Greig, P. Veillet, and E. Kolb, J. Magn. Magn. Mater. **156**, 379 (1996).
[7] J. Xu, M. A. Howson, B. J. Hickey, D. Greig, E. Kolb, P. Veillet, and N. Wiser, Phys. Rev. B **55**, 416 (1997).
[8] M. Shima, L. G. Salamanca-Riba, R. D. McMichael, and T. P. Moffat, J. Electrochem. Soc. **149**, C439 (2002).
[9] I. Bakonyi, J. Tóth, L. F. Kiss, E. Tóth-Kádár, L. Péter, and A. Dinia, J. Magn. Magn. Mater. **269**, 156 (2004).
[10] I. Bakonyi, L. Péter, Z. Rolik, K. Kiss-Szabó, Z. Kupay, J. Tóth, L. F. Kiss, and J. Pádár, Phys. Rev. B **70**, 054427 (2004).
[11] N. Wiser, J. Magn. Magn. Mater. **159**, 119 (1996).
[12] B. J. Hickey, M. A. Howson, S. O. Musa, and N. Wiser, Phys. Rev. B **51**, 667 (1995).
[13] T. R. McGuire and R. I. Potter, IEEE Trans. Magn. **11**, 1018 (1975).
[14] V. Weihnacht, L. Péter, J. Tóth, J. Pádár, Zs. Kerner, C. M. Schneider, and I. Bakonyi, J. Electrochem. Soc. **150**, C507 (2003).
[15] I. Bakonyi, L. Péter, V. Weihnacht, J. Tóth, L. F. Kiss, and C. M. Schneider, J. Optoelectron. Adv. Mater. **7**, 589 (2005).
[16] L. Péter, Á. Cziráki, L. Pogány, Z. Kupay, I. Bakonyi, M. Uhlemann, M. Herrich, B. Arnold, T. Bauer, and K. Wetzig, J. Electrochem. Soc. **148**, C168 (2001).
[17] L. Péter, Q. X. Liu, Zs. Kerner, and I. Bakonyi, Electrochim. Acta **49**, 1513 (2004).
[18] Á. Cziráki, L. Péter, V. Weihnacht, J. Tóth, E. Simon, J. Pádár, L. Pogány, C. M. Schneider, T. Gemming, K. Wetzig, G. Tichy, and I. Bakonyi, J. Nanosci. Nanotechnol. (to be published).
[19] D. Barlett, F. Tsui, D. Glick, L. Lauhon, T. Mandrekar, C. Uher, and R. Clarke, Phys. Rev. B **49**, 1521 (1994).
[20] R. Clarke, D. Barlett, F. Tsui, B. X. Chen, and C. Uher, J. Appl. Phys. **75**, 6174 (1994).
[21] J. Crangle and G. M. Goodman, Proc. R. Soc. London, Ser. A **321**, 477 (1971).
[22] Q. X. Liu, L. Péter, J. Tóth, L. F. Kiss, Á. Cziráki, and I. Bakonyi, J. Magn. Magn. Mater. **280**, 60 (2004).
[23] M. Prutton, *Thin Ferromagnetic Films* (Butterworths, London, 1964).
[24] T. B. Massalski, ed., *Binary Alloy Phase Diagrams*, 2nd ed. plus updates on CD-ROM (ASM International, Materials Park, Ohio, 1996).
[25] J. R. Childress and C. L. Chien, Phys. Rev. B **43**, 8089 (1991).
[26] D. Kechrakos and K. N. Trohidou, Phys. Rev. B **62**, 3941 (2000).
[27] P. Allia, M. Coisson, P. Tiberto, F. Vinai, M. Knobel, M. A. Novak, and W. C. Nunes, Phys. Rev. B **64**, 144420 (2001).
[28] Q. X. Liu, L. Péter, J. Pádár, and I. Bakonyi, J. Electrochem. Soc. **152**, C316 (2005).
[29] J. C. Slonczewski, J. Appl. Phys. **73**, 5957 (1993).
[30] G. J. Gutierrez, R. Selestino, R. A. Mayanovic, and G. A. Prinz,

J. Appl. Phys. **81**, 5352 (1997); J. J. de Vries, G. J. Strijkers, M. T. Johnson, A. Reinders, and W. J. M. de Jonge, J. Magn. Magn. Mater. **148**, 187 (1995).

[31] R. H. Kodama, A. E. Berkowitz, E. J. McNiff, Jr., and S. Foner, Phys. Rev. Lett. **77**, 394 (1996); A. E. Berkowitz, R. H. Kodama, S. A. Makhlouf, F. T. Parker, F. E. Spada, E. J. McNiff Jr., and S. Foner, J. Magn. Magn. Mater. **196**, 591 (1999).

[32] M. J. Hall, B. J. Hickey, M. A. Howson, M. J. Walker, J. Xu, D. Greig, and N. Wiser, Phys. Rev. B **47**, 12785 (1993).

[33] X. W. Zhou, H. N. G. Wadley, R. A. Johnson, D. J. Larson, N. Tabat, A. Cerezo, A. K. Petford-Long, G. D. W. Smith, P. H. Clifton, R. L. Martens, and T. F. Kelly, Acta Mater. **49**, 4005 (2001).

[34] C. B. Ene, G. Schmitz, R. Kirchheim, and A. Hütten, Acta Mater. **53**, 3383 (2005).